

Received September 21, 2017, accepted October 13, 2017, date of publication October 17, 2017, date of current version April 4, 2018.

Digital Object Identifier 10.1109/ACCESS.2017.2763898

Dark Image Enhancement Using Perceptual Color Transfer

JONATHAN CEPEDA-NEGRETE¹, RAUL E. SANCHEZ-YANEZ², (Member, IEEE),
FERNANDO E. CORREA-TOME², AND ROCIO A. LIZARRAGA-MORALES³, (Member, IEEE)

¹Department of Agricultural Engineering, University of Guanajuato DICIVA, Irapuato, Gto. 36500, Mexico

²Department of Electronics Engineering, University of Guanajuato DICIS, Salamanca, Gto. 36885, Mexico

³Department of Multidisciplinary Studies, University of Guanajuato DICIS, Yuriria, Gto. 38944, Mexico

Corresponding author: Raul E. Sanchez-Yanez (sanchezzy@ugto.mx)

The work of J. Cepeda-Negrete was supported by the Mexican National Council on Science and Technology (CONACyT) through the Scholarship 290747 under Grant 388681/254884.

ABSTRACT In this paper, we introduce an image enhancing approach for transforming dark images into lightened scenes, and we evaluate such method in different perceptual color spaces, in order to find the best-suited for this particular task. Specifically, we use a classical color transfer method where we obtain first-order statistics from a target image and transfer them to a dark input, modifying its hue and brightness. Two aspects are particular to this paper, the application of color transfer on dark imagery and in the search for the best color space for the application. In this regard, the tests performed show an accurate transference of colors when using perceptual color spaces, being RLAB the best color space for the procedure. Our results show that the methodology presented in this paper can be a good alternative to low-light or night vision processing techniques. Besides, the proposed method has a low computational complexity, property that is important for real time applications or for low-resource systems. This method can be used as a preprocessing step in order to improve the recognition and interpretation of dark imagery in a wide range of applications.

INDEX TERMS Perceptual color space, color transfer, dark image enhancement, night vision.

I. INTRODUCTION

Image enhancement is a challenging task in the image processing field. The objective of image enhancement algorithms is to improve the quality and to ease the visibility of a given image, e.g. an image with noise, an image with low contrast, or a dark image. With such improvement, images are more useful in application fields like human understanding, digital photography [1], medical image analysis [2], object detection [3], face recognition [4], and video surveillance [5].

Dark images, or images taken under low light conditions, are problematic because of their narrow dynamic range. Under these conditions, a regular camera sensor introduces significant amounts of noise, further reducing the information content in the image. Because of these limitations, dark image enhancement algorithms occasionally produce artifacts in the processed images [6]. One traditional approach to dark image enhancement is to use monochromatic representations and ignore the color features. However, color images have numerous benefits over monochromatic images for surveillance and security applications [7]–[10]. Moreover, a color

representation may facilitate the recognition of night vision imagery and its interpretation [8].

Most of classical methods that have been used over decades for dark image enhancement are histogram-based; for example, histogram stretching, histogram equalization, brightness preserving bi-histogram equalization [11], contrast limited adaptive histogram equalization [12], [13], to mention a few. The aforementioned methods have been categorized as direct and indirect methods [14]. Direct methods consist of improving image contrast by optimizing an objective contrast measure. Indirect methods exploit the dynamic range without using a contrast measure. However, the performance of such histogram-based algorithms is very limited with color images because these methods change the correlation between the color components of the original scene. Most recently, a number of methods for improving the contrast using a global mapping from feature analysis have been published specially oriented to video enhancement [15], [16].

Color constancy approaches are also used to increase the overall luminance in the image. Although color constancy

algorithms have been originally developed to estimate the color of a light source by discarding the illuminant from the scene, they also improve the chromatic content [17]. Some works have explored the use of color constancy algorithms for color image enhancement purposes [18], [19]. In particular, [18] was oriented to local contrast enhancement using the White-Patch and the Gray-World algorithms in combination with an automatic color equalization technique. In this work, and just for comparison purposes, we have included the two aforementioned color constancy algorithms to enhance dark images.

Image fusion is another approach used to enhance dark images. This technique increases the visual information in an image by combining different bands or images into the RGB space [9], [10], [20]. In image fusion, generally two monochromatic images from different spectral bands are used. A near-infrared or a visible image is considered as the R component, and a thermal image is designated as the G component [8], [21]. This combination of bands is used to build a look-up table (LUT) to transfer colors to other images. However, this scheme may produce images with false colors (i.e. colors that are not actually in the scene). These false colors could also diminish the scene comprehension [22], [23].

Color transfer (a.k.a. color mapping) is an efficient approach to enhance an image under low light conditions avoiding false colors. This technique recolors an input image by transferring the color content from another image used as a reference (target). There are three main strategies used for color transfer between images: geometric-based methods, user-aided solutions, and statistical approaches. In geometric-based methods [24], the transfer of aspects of color rendition from one image to another can be facilitated by searching for corresponding features that are depicted in both images. By actively finding correspondences between pairs of images, the color transfer algorithm can better ensure that features that occur in both images end up having the same colors. When the structure and content of the input image is very different from the target image, many automatic methods will fail to find a successful mapping. In such cases, it may be required the application of an input from the user in order to guide the correspondences between the source and reference; these methods are referred to as user-aided solutions [25]–[27]. When direct correspondences between image features are not available, approaches using statistical properties are often used to define a mapping between the two images [28]–[34]. Concerning the problem of false colors, different studies have addressed the correction of unreal appearance using color transfer techniques [8], [22], [35], [36]. Such works have been specifically oriented to tasks like scene segmentation and classification [37], [38]. If designed properly, the color transfer applied to dark imagery improves the ability of an observer to understand a scene [37]. Notice that most of color transfer methods were developed using the $l\alpha\beta$ color space, remaining unstudied the performance using other color spaces.

In this work, we propose the applicability of a well-known statistical method for color transfer [28], now using the color mapping to transform dark images into daylight-looking images. Few previous works already have studied night-time imagery enhancement. However, images used in those studies are professional landscapes with a controlled exposure [39], [40], or they were created by the fusion of images from different spectral or color bands [8], [41]–[43]. Our approach uses only a single image which is completely dark (without adjusted exposure), and obtained from a common RGB-CCD sensor. Furthermore, most of the color transfer research has been performed using the $l\alpha\beta$ color space; few studies have been focused on other perceptual spaces and none on RLAB space. In this study, we propose to apply the color transfer using RGB and four perceptual color spaces: $l\alpha\beta$, CIELUV, CIELAB and RLAB. The latter color space, designed specifically to emulate the human perception of color under extreme light conditions [44]. Dark or night imagery can be included in such kind of conditions. The performance of the color transfer using all color spaces is compared. Additionally, we include in the comparison the results yielded by image enhancement methods used as reference. Tests are conducted in order to support our hypothesis: better results are obtained when the color transfer is performed on the RLAB space.

The rest of this article is organized as follows. The proposed framework is presented in Section II, including the description of the color spaces considered, the formulation of the color transfer function, and the method used to assess the correct color transfer. Experimental results are discussed in Section III, followed by the concluding remarks in Section IV.

II. METHODOLOGY

This section introduces the perceptual color transfer (PCT) technique used in this work to transform a dark image into a lightened scene. We use a classical color transfer technique to perform this transformation [28]. Although there are many color transfer approaches, this method was chosen because of its simplicity and speed. Figure 1 shows the color transfer procedure performed using this technique. Notice that the images used in this study are obtained from a common RGB-CCD sensor. The details regarding the methodology are described in the following subsections.

A. COLOR TRANSFER USING FIRST ORDER STATISTICS

A color transfer method aims to modify the color content of a given image by transferring the statistics from a reference image. In this study, we use a classical method, proposed by Reinhard *et al.* [28]. In this method, only the global mean and the standard deviation in the image are calculated. The aim of our work is to transform an input image (dark) into another with a look similar to that of the reference image (target). Specifically, modifying the color content of the dark image using the statistics from the target image. This procedure may be improved by using a different color space. After a

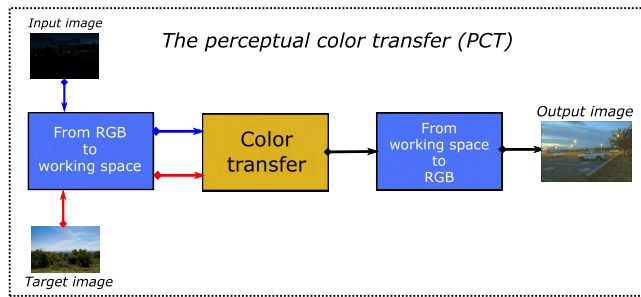


FIGURE 1. Color transfer procedure upon a dark image.

conversion of both images from RGB to that color space, the statistics are calculated for each color channel and for both images, the dark and the target one. The mean and standard deviation are calculated using Eqs. (1)–(4).

$$\mu_i^D = \frac{1}{M_D N_D} \sum_{x=1}^{M_D} \sum_{y=1}^{N_D} D_i(x, y), \quad (1)$$

$$\mu_i^T = \frac{1}{M_T N_T} \sum_{x=1}^{M_T} \sum_{y=1}^{N_T} T_i(x, y), \quad (2)$$

$$\sigma_i^D = \sqrt{\frac{1}{M_D N_D} \sum_{x=1}^{M_D} \sum_{y=1}^{N_D} (D_i(x, y) - \mu_i^D)^2}, \quad (3)$$

$$\sigma_i^T = \sqrt{\frac{1}{M_T N_T} \sum_{x=1}^{M_T} \sum_{y=1}^{N_T} (T_i(x, y) - \mu_i^T)^2}, \quad (4)$$

where μ_i and σ_i are the mean and standard deviation, i is the channel index, M is the number of rows, and N is the number of columns of the image. Here, the signals D and T correspond to the dark and target images, respectively.

The color transfer between the target and the input images for the channel i is performed using the Eq. (5)

$$O_i(x, y) = \frac{\sigma_i^T}{\sigma_i^D} (D_i(x, y) - \mu_i^D) + \mu_i^T, \quad (5)$$

where O represents the output image in the transfer. Finally, we transform the O image back to RGB using the inverse transformation.

Notice that for a given image, the color components are processed separately. If a color space different than RGB is used, the RGB image needs to be transformed to that color space before performing the color transfer. Then, the image is transformed back to RGB to display the results.

B. COLOR TRANSFER IN THE RLAB PERCEPTUAL COLOR SPACE

The classical color transfer was originally applied in the $l\alpha\beta$ color space, and several works have adopted this approach [22], [45], [46]. Reinhard and Pouli [39] performed a comparison of color spaces, finding that the use of the

CIELAB color space is also recommended for color transfer using natural low-light images.

In this work, we explore the usage of color transfer for completely dark images. Therefore, we performed tests using five color spaces. The color spaces used in this study are: RGB, $l\alpha\beta$, CIELUV, CIELAB and RLAB. Other color spaces were also considered. However, preliminary results showed that those spaces are not adequate for our application. The Table 1 shows the image components with their corresponding index i (see Eqs. (1)–(4)) for each color space used.

TABLE 1. The components corresponding to the index i according to each color space.

| Color space | index i |
|----------------|------------------------------|
| RGB | $i \in \{R, G, B\}$ |
| $l\alpha\beta$ | $i \in \{l, \alpha, \beta\}$ |
| CIELUV | $i \in \{l, u, v\}$ |
| CIELAB | $i \in \{l, a, b\}$ |
| RLAB | $i \in \{l, a, b\}$ |

RGB is the first space that has been included for comparison purposes. The second color space considered is the $l\alpha\beta$, inspired from previous studies [23], [28]. The third is the CIE 1976 (L, u^*, v^*) color space, commonly known as CIELUV, and the fourth is the CIE 1976 (L, a^*, b^*) color space, better known as CIELAB. For these later two spaces, the Euclidean distance between two points in the space is proportionally uniform to the perceptual difference of the corresponding colors at the points. Finally, the fifth space under evaluation is the RLAB, which was originally designed in order to fix the problems shown by CIELAB, under unusual lighting conditions [44]. RLAB maintains perceptual properties under normal light conditions (natural light), and also under extreme conditions. Dark-time imagery are an example of such extreme cases.

The procedure to convert an image from RGB to RLAB is included here for clarity sake. To transform an RGB image to perceptual color spaces, the data are first transformed to the CIEXYZ color space [47]. In order to transform an image from RGB into CIEXYZ, the RGB space needs to be defined. Here, sRGB is used because it is based in a colorimetric RGB calibrated space [48]. The Eq. (6) is used to perform the transformation

$$\begin{bmatrix} X \\ Y \\ Z \end{bmatrix} = \begin{bmatrix} 0.4124 & 0.3576 & 0.1805 \\ 0.2126 & 0.7152 & 0.0722 \\ 0.0193 & 0.1192 & 0.9505 \end{bmatrix} \begin{bmatrix} r \\ g \\ b \end{bmatrix}, \quad (6)$$

where $r, g, b \in [0, 1]$, obtained by dividing each R, G, B component by 255. After, the main equations used to obtain the transformation from XYZ to RLAB are given in Eqs. (8)–(11). For further details, please refer to the work of Fairchild [44].

$$\text{RAM} = \begin{bmatrix} 1.0020 & -0.0401 & 0.0084 \\ -0.0042 & 0.9666 & 0.0008 \\ 0.0000 & 0.0000 & 0.9110 \end{bmatrix}, \quad (7)$$

$$\begin{bmatrix} X_{ref} \\ Y_{ref} \\ Z_{ref} \end{bmatrix} = \mathbf{RAM} \begin{bmatrix} X \\ Y \\ Z \end{bmatrix}, \quad (8)$$

$$L^R = 100(Y_{ref})^\sigma, \quad (9)$$

$$a^R = 430[(X_{ref})^\sigma - (Y_{ref})^\sigma], \quad (10)$$

$$b^R = 170[(Y_{ref})^\sigma - (Z_{ref})^\sigma]. \quad (11)$$

In this study, $\sigma = 1/3.5$ is used. This value is suggested for images under very low luminance conditions [44]. The inverse transformation required to go back to XYZ is given by the following equations

$$Y_{ref} = \left(\frac{L^R}{100}\right)^{1/\sigma}, \quad (12)$$

$$X_{ref} = \left[\left(\frac{a^R}{430}\right) + (Y_{ref})^\sigma\right]^{1/\sigma}, \quad (13)$$

$$Z_{ref} = \left[(Y_{ref})^\sigma - \left(\frac{b^R}{170}\right)\right]^{1/\sigma}, \quad (14)$$

$$\begin{bmatrix} X \\ Y \\ Z \end{bmatrix} = (\mathbf{RAM})^{-1} \begin{bmatrix} X_{ref} \\ Y_{ref} \\ Z_{ref} \end{bmatrix}. \quad (15)$$

Finally, the inverse transformation, from CIEXYZ to RGB is given in Eq. (16)

$$\begin{bmatrix} r \\ g \\ b \end{bmatrix} = \begin{bmatrix} 3.2410 & -1.5374 & -0.4986 \\ -0.9692 & 1.8760 & 0.0416 \\ 0.0556 & -0.2040 & 1.0570 \end{bmatrix} \begin{bmatrix} X \\ Y \\ Z \end{bmatrix}. \quad (16)$$

The equations for the color spaces $\alpha\beta$, CIELUV and CIELAB can be consulted in the Appendix section.

C. ASSESSMENT OF THE COLOR TRANSFER

An important problem regarding to image processing methodologies is the comparison of images. When different algorithms are applied to an image, an objective measure is necessary to compare the outcomes. In this study, we use a metric for assessing the quality of the image, by calculating the similarity between the outcome and the target image. These distance metrics have already been used for quality assessment in a previous work [49].

The comparison measure uses the histograms of the images (a histogram with 255 bins for each component), calculating the distance between them. To corroborate the consistency of the comparisons, we tested three different distances between histograms of the outcome and target images: euclidean (d_{L_2}), Bhattacharyya (d_B) [50] and chi-square (d_{chi-s}).

$$d_{L_2}(h_o, h_t) = \sqrt{\sum_j (h_o(j) - h_t(j))^2}, \quad (17)$$

$$d_B(h_o, h_t) = \sqrt{1 - \frac{1}{\sqrt{\mu_{h_o}\mu_{h_t}N^2}} \sum_j \sqrt{h_o(j) \cdot h_t(j)}}, \quad (18)$$

$$d_{chi-s}(h_o, h_t) = \sum_j \frac{(h_o(j) - h_t(j))^2}{h_o(j)}, \quad (19)$$

where h_o and h_t are the normalized color histograms from the output image, and from the target image, respectively. For the euclidean, Bhattacharyya and chi-square (d_{L_2} , d_B , d_{chi-s}) distances, a small distance value corresponds to a better color transfer. In comparison tests, the intersection (d_\cap) measure is also considered,

$$d_\cap(h_o, h_t) = \sum_j \min(h_o(j), h_t(j)), \quad (20)$$

where the higher the value, the better the color transfer is.

III. EXPERIMENTAL RESULTS

The experiments were performed using different approaches for the enhancement of a dark image given as input to our system. On one hand and for comparison purposes, three methods are used to enhance this input without the need of any reference image. These methods are the White Patch algorithm (WP), the Gray-World algorithm (GW), and the Histogram Equalization (HE). On the other hand, outcomes are obtained using the color transfer from a specific target image into the same input. This latter procedure is made in RGB and each one of the perceptual color spaces under discussion: $\alpha\beta$, CIELUV, CIELAB and LAB. Figure 2 depicts the proposed methodology comparing different approaches.

It is important to mention that additional experiments were performed using other non perceptual color spaces, HSI, YIQ, YCbCr and the opponent color space ($O_1O_2O_3$). However, we obtained poor results using these spaces and for that reason the corresponding results are not reported in this work.

As far as we know, there are no reference databases for this particular purpose (images under total darkness), hence the experiments are carried out in two ways. Firstly, we provide a dark imagery dataset consisting of 200 RGB images, obtained using an off-the-shelf camera. Secondly, we transform the well-known BSDS300 database [51] into a night-time image set using the methodology proposed by Thompson *et al.* [52]. Both sets of images are available in [53] and [54].

A. EXPERIMENT 1: NATURAL NIGHT-TIME IMAGERY

As a first experiment, we propose a collection of dark images taken with an off-the-shelf camera. The image database used consists of a collection of 200 dark images. The image set was taken under dark light conditions or under the moonlight. Additionally, we chose 10 target images from the BSDS300 database: 2092, 35010, 35058, 95006, 100080, 108005, 113044, 124084, 143090 and 232038. This selection was made arbitrarily according to the variation in their color content. The experiment consists of the color transfer between the darkened image and its corresponding original natural scene using the aforementioned color spaces. Additionally, WP, GW and the HE are used as reference methods. An example out of the 200 dark images, from this first experiment, is depicted in Figure 3. Visually we can appreciate that the best outcomes are obtained using perceptual color spaces. However, it is important to analyze numerically the metrics in order to determine the best one. A test series was performed

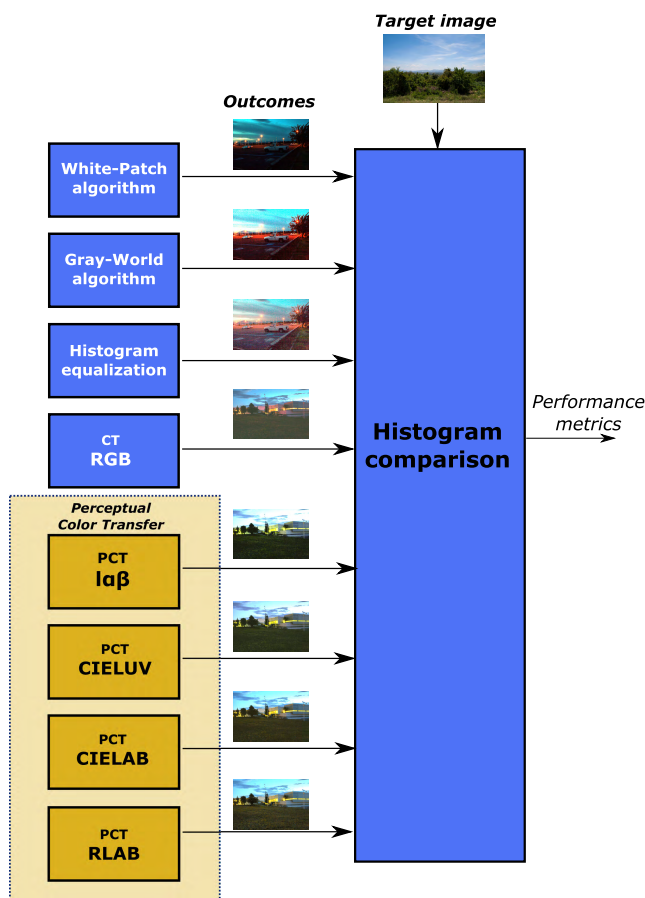


FIGURE 2. Diagram of the methodology followed for performance comparison.

TABLE 2. As an example of distance measures between the target (Figure 3b) and the outcomes after processing the input (Figure 3-a) using the different approaches (Figure 3-(c-j)).

| Method | euclidean | Bhattacharyya | chi-s | intersection |
|-----------------------|--------------|---------------|--------------|--------------|
| WP | 3.815 | 0.755 | 196.600 | 0.438 |
| GW | 4.386 | 0.850 | 228.865 | 0.206 |
| HE | 4.275 | 0.803 | 460.569 | 0.314 |
| CT _{RGB} | 3.63 | 0.591 | 14.641 | 0.646 |
| PCT _{Iαβ} | 2.596 | 0.360 | 13.001 | 1.224 |
| PCT _{CIELUV} | 2.261 | 0.190 | 6.105 | 1.522 |
| PCT _{CIELAB} | 2.172 | 0.006 | 4.978 | 1.589 |
| PCT _{RLAB} | 2.155 | 0.000 | 4.949 | 1.604 |

measuring the distance between two histograms. A histogram corresponding to the original natural image and the other to the outcome.

Continuing with the same example. The Table 2 presents the results obtained from the image No. 92 shown in Figure 3. Each cell in this table shows the comparison value between the outcome and the target image given in Figure 3b. Each value is obtained using an enhancement method and a specific distance metric. This table shows that without exception, the best values are obtained using RLAB. Additionally, we can appreciate that the color transfer in RGB is worse than the results obtained using perceptual color spaces.

Although these comments apply only for the particular example, further exhaustive experimentation was done in order to obtain general conclusions. Such conclusions will be given from the reproduction of each input-target pair using different target images. Figure 4 shows an example of the outcomes obtained from a single input image after applying six different targets. The color transfer is made in the RLAB color space. The figure shows some target images highly dissimilar to the input scene, leading to the generation of false colors in the outcomes. Although this feature could be useful in particular applications (e.g. generation of artistic effects), it is not desirable for our purposes.

The color transfer was applied to the 200 dark images, using for each image all the 10 targets. The distance measures were computed for all the outcome-target pairs. A total of 2000 outcomes were obtained for each color transfer method and for each color space, 2000 measures for each reference method. Afterward, the mean value from the 2000 measures was computed for each approach under evaluation. In Table 3, the cells show the mean value for each approach, and for each distance measure and, we can appreciate that the PCT in the RLAB space is the best approach for the whole set of images.

TABLE 3. Mean values from the 2000 measures for each method under analysis. Data are given for the four metrics of distance between histograms.

| Method | euclidean | Bhattacharyya | chi-s | intersection |
|-----------------------|--------------|---------------|---------------|--------------|
| WP | 4.124 | 0.826 | 1670.527 | 0.265 |
| GW | 4.287 | 0.863 | 844.202 | 0.150 |
| HE | 4.074 | 0.898 | 2072.574 | 0.128 |
| CT _{RGB} | 4.194 | 0.716 | 60.984 | 0.377 |
| PCT _{Iαβ} | 3.898 | 0.627 | 86.404 | 0.550 |
| PCT _{CIELUV} | 3.900 | 0.633 | 58.397 | 0.549 |
| PCT _{CIELAB} | 3.890 | 0.625 | 63.158 | 0.555 |
| PCT _{RLAB} | 3.885 | 0.624 | 56.428 | 0.557 |

B. EXPERIMENT 2: NIGHT BSDS300 DATASET

In this experiment, we transform the widely known BSDS300 database [51] into a night-time image set using the framework proposed by Thompson *et al.* [52]. This methodology emulates loss-of-detail and noisy effects associated with night vision assuming the input as an RGB image. If our source image is a colorful image, first a dark tone should be mapped. Thus, the image is mapped to a scene with night lighting, where each pixel is a single number indicating the “brightness” of the pixel as seen at night. This will tend to bluish hue because the rods in the human eye are more sensitive to blues than to greens and reds [52]. Afterwards, a filtering stage is carried out in order to simulate loss of visual acuity. One way of achieving this, is using an anisotropic diffusion, which has the effect of smoothing the geometry of edges without blurring across the edges. Finally, an amount of Gaussian noise is applied to the images because an actual night image presents overly noise depending the sensor. Figure 5 shows three examples of the transformed BSDS300 dataset.

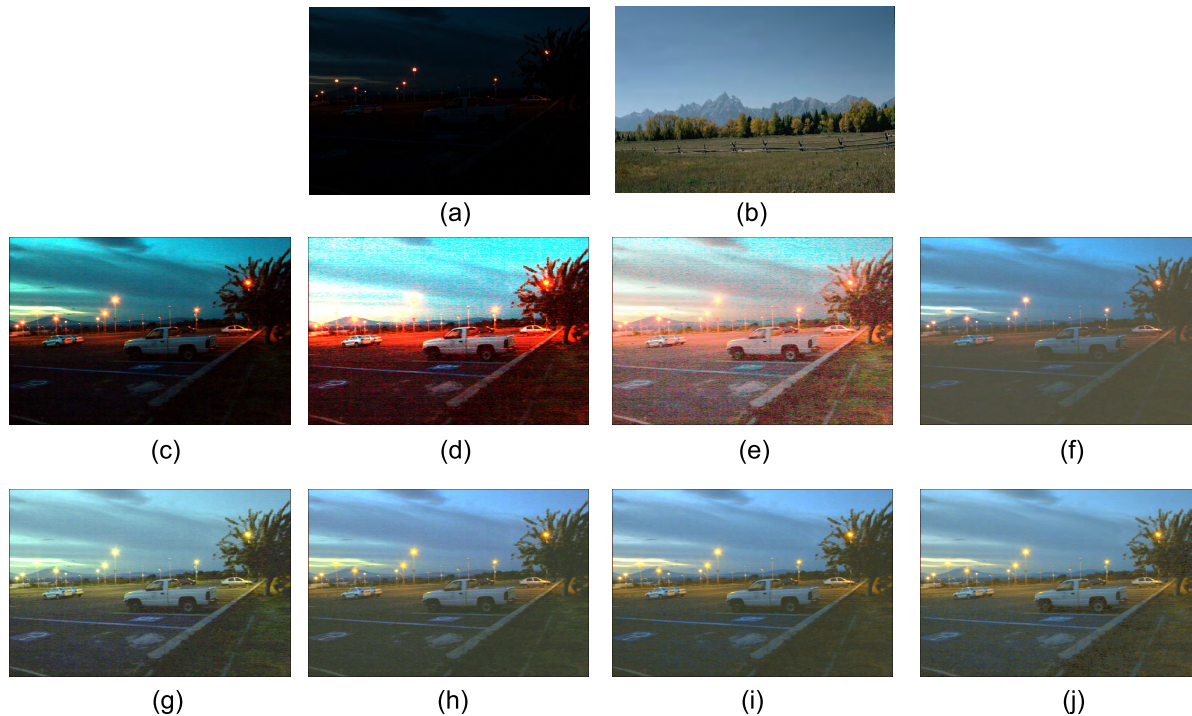


FIGURE 3. A sample out of the 200 dark images and its enhanced outcomes obtained using different methods. In (a) the input no. 92 (landscape); (b) the target image BSDS300 No. 2092; outcomes using (c) WP, (d) GW, and (e) Histogram equalization; outcomes using (b) as target and (f) CT in RGB, (g) PCT in $I\alpha\beta$, (h) PCT in CIELUV, (i) PCT in CIELAB, and (j) PCT in RLAB.

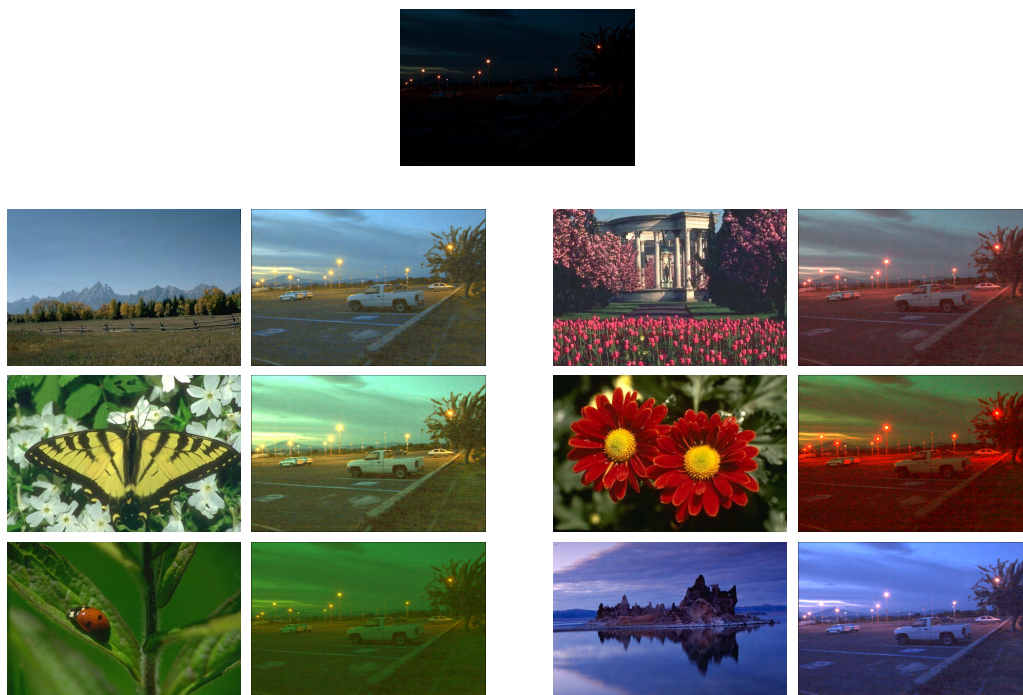


FIGURE 4. Examples of the corresponding outcomes of the color transfer using a different target image.

In this second experiment the color transfer was applied to the 300 darkened images, using their corresponding original scene as target. A sample out of the 300 darkened images,

from this second experiment, is depicted in Figure 6. Similarly to the first experiment, a test series was carried out for obtaining the four distances. Table 4 provides the quantitative

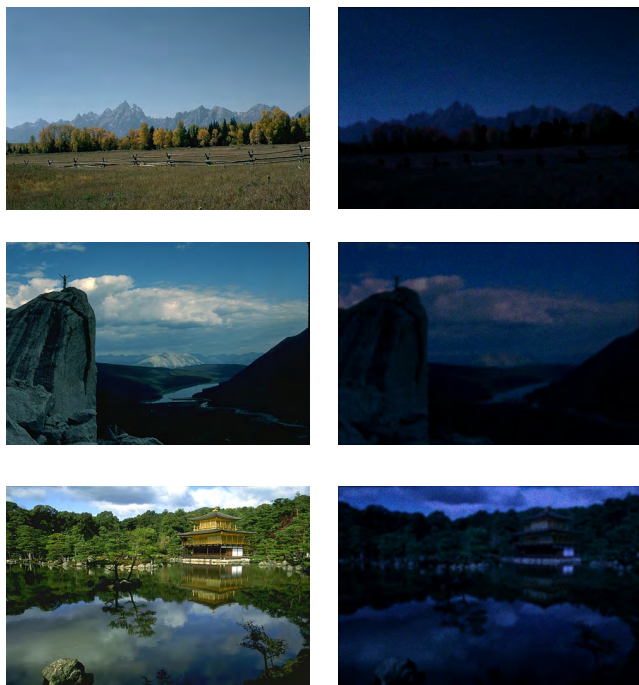


FIGURE 5. Three samples of the new darkened BSDS300 dataset: 2092, 14037 and 65010 images, respectively.

TABLE 4. As an example, distance measures between the original image 65010 (Figure 6b) and the outcomes after processing the darkened input (Figure 6a) using the different approaches (Figure 6c-j).

| Method | euclidean | Bhattacharyya | chi-s | intersection |
|---------------------------|--------------|---------------|--------------|--------------|
| WP | 2.481 | 0.488 | 1766.438 | 1.246 |
| GW | 3.180 | 0.615 | 1725.54 | 0.642 |
| HE | 3.448 | 0.688 | 31.635 | 0.513 |
| CT _{RGB} | 2.455 | 0.395 | 9.033 | 1.229 |
| PCT _{<i>lαβ</i>} | 1.176 | 0.159 | 3.522 | 2.118 |
| PCT _{CIELUV} | 0.863 | 0.057 | 1.456 | 2.390 |
| PCT _{CIELAB} | 0.792 | 0.012 | 1.390 | 2.435 |
| PCT _{RLAB} | 0.662 | 0.000 | 1.461 | 2.506 |

results, obtained from the sample image shown in Figure 6. This table shows that according to euclidean, Bhattacharyya and intersection distances, the best values are obtained using RLAB. Only the chi-s distance shows that the method using CIELAB is the best, however using RLAB the value is just marginally lower.

The distance measures were computed for all the outcome-target pairs. A total of 300 outcomes were obtained for each color transfer method and for each color space (RGB, $l\alpha\beta$, CIELUV, CIELAB or RLAB). Additionally, the outcomes from the reference methods were compared with the corresponding target image, obtaining 300 measures for each reference method (WP, GW and histogram equalization). Afterward, the mean value from the 300 measures was calculated for each approach under evaluation. In Table 5, the cells show the mean value for each approach, and for each distance measure. Consistently, the mean values show that the color transfer using the RLAB space is our best option in order to obtain the best mapping.

TABLE 5. Mean values from the 300 measures for each method under analysis. Data are given for the four metrics of distance between histograms.

| Method | euclidean | Bhattacharyya | chi-s | intersection |
|---------------------------|--------------|---------------|--------------|--------------|
| WP | 3.134 | 0.611 | 826.140 | 0.821 |
| GW | 3.455 | 0.699 | 924.531 | 0.559 |
| HE | 3.579 | 0.686 | 105.761 | 0.523 |
| CT _{RGB} | 2.651 | 0.364 | 15.835 | 1.195 |
| PCT _{<i>lαβ</i>} | 1.079 | 0.051 | 14.869 | 2.264 |
| PCT _{CIELUV} | 1.041 | 0.053 | 5.725 | 2.294 |
| PCT _{CIELAB} | 0.916 | 0.031 | 3.225 | 2.380 |
| PCT _{RLAB} | 0.879 | 0.022 | 3.386 | 2.400 |

TABLE 6. Comparison of the PSNR average for each approach in the whole BSD300 dataset. PCT_{RLAB} obtained the highest value, meaning that this approach produces less noise than the other.

| Approach | PSNR (dB) |
|---------------------------|---------------|
| Night | 9.097 |
| WP | 12.946 |
| GW | 12.370 |
| HE | 13.008 |
| CT _{RGB} | 19.894 |
| PCT _{<i>lαβ</i>} | 20.550 |
| PCT _{CIELUV} | 20.878 |
| PCT _{CIELAB} | 21.370 |
| PCT _{RLAB} | 21.494 |

We have found that applying the color transfer methodology in a perceptual color space is appreciably better than applying it in the RGB color space. From all the methods, color transfer using RLAB always attains the best results, for each distance metrics used. Additionally to this test series, we performed a statistical significance z-test between the results obtained using the RLAB and the CIELAB spaces, finding that the difference is significant using 95% as confidence level. We may conclude that the color transfer in the RLAB color space is the best choice for the enhancement of dark images given a target color content.

C. COMMENTS ON NOISE ISSUES

Although this work is focused on the emulation of colors and the assessment of this task on several color spaces, we need to take into account that the enhancement of dark images also amplifies the noise existent on them. Here we include a brief discussion in this regard.

In an additional test of noise reduction, we measured the PSNR (Peak Signal to Noise Ratio) in those images generated in the Experiment 2. We used this dataset because the PSNR measure between the different outcomes and the original scene are computed for comparative purposes. Such original image is the one in daylight, before the darkening, blur and noise addition procedures.

Noticing that the higher the PSNR value is the better the quality of the lightening procedure is, in Table 6 we can find the averages of the PSNR for each approach over the whole set of 300 images. It is possible to appreciate that the best value corresponds to the PCT approach in the RLAB space. A qualitative example for an image out of the 300 is given in Figure 6, showing the particular PSNR

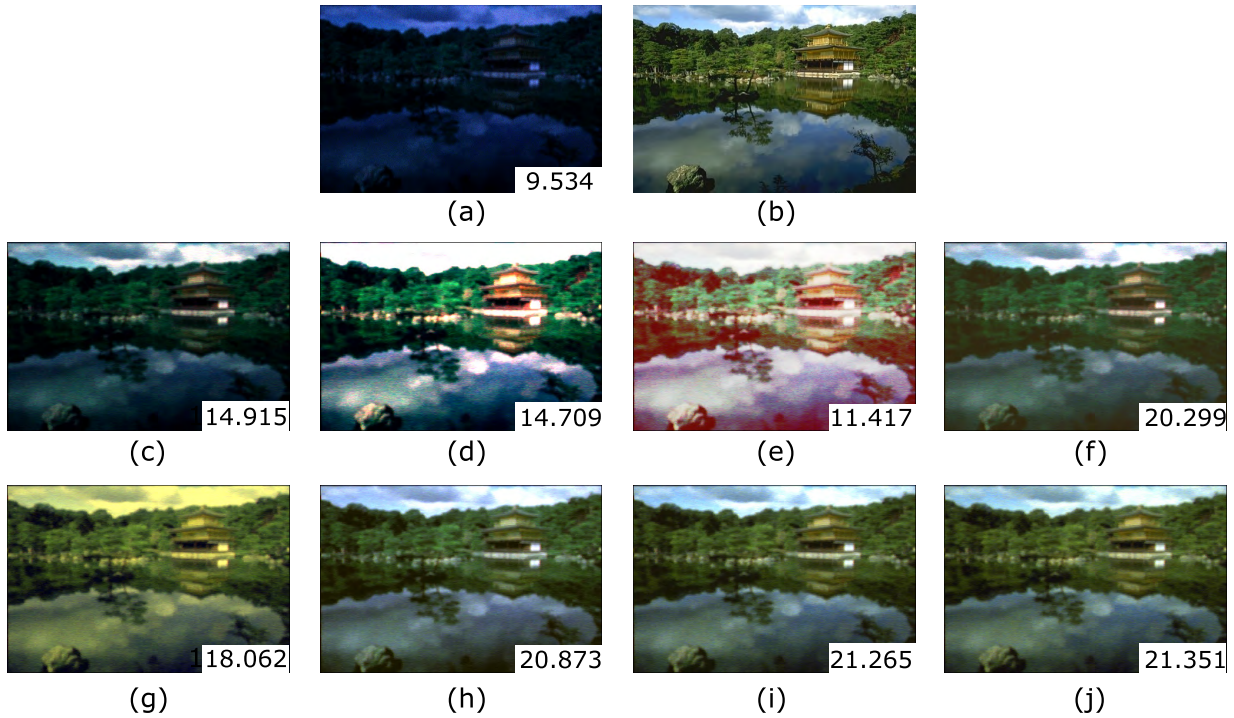


FIGURE 6. A sample out of the 300 images from the new darkened BSDS300 dataset and enhanced outcomes obtained using different methods. In (a) the night image 65010; (b) its corresponding original image; outcomes using (c) WP, (d) GW, and (e) Histogram equalization; outcomes using (b) as target and (f) CT in RGB, (g) PCT in $l\alpha\beta$, (h) PCT in CIELUV, (i) PCT in CIELAB, and (j) PCT in RLAB. PSNR value is also included in the box of each outcome representing the noise level presented.

results for this sample. In this case, and in accordance with the average results over the whole set, the PT in RLAB yields the best PSNR value. In general, we can say that PCT in the RLAB space produces the best natural color transfer and, in a collateral way, also reduces the presence of noise.

If additional noise reduction is required, a number of filters, ranging from the basic mean and median to more specific ones [55], can be applied after our approach, improving this way the look of the image. Figure 7 shows the two samples used as qualitative examples of our experiments. The reference (original) images are presented in (a) and outcomes of the color transfer in RLAB are depicted in (b); finally, in (c) are shown outcomes from (b) after using successively two 3×3 filters, first a mean filter and then a median one. In the figure we can appreciate that the filtered outcomes attain a higher PSNR value.

IV. CONCLUDING REMARKS

In this study, we have discussed an image processing-based approach to transform dark-time imagery into scenes with a daylight appearance. This approach uses a single input color image, captured by an off-the-shelf camera. Our main contribution is the use of color transfer in a new way to lighten dark images, taking advantage of the property of the color transfer methodologies to diminish the production of unnatural colors. The experimental results show that, in general, the color transfer in perceptual spaces yields better results than the

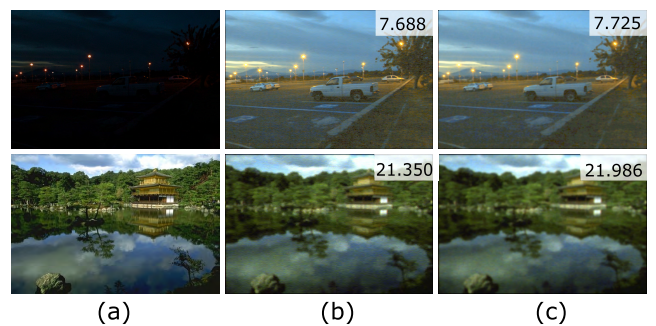


FIGURE 7. The two examples used in our experiments. (a) Original images. (b) Outcomes from the color transfer in RLAB space. (c) The same outcomes after a filtering stage. Additionally, PSNR value of the comparison between the original and the outcome images is included.

color transfer in RGB. Besides, the color transfer applied to images in the RLAB space attains the best results. We have also proposed a dataset of night-time imagery, as benchmark for future studies in the field and, the modification of another widely known dataset artificially darkened. This study may be applied to improve the recognition and interpretation of night-time imagery, in tasks such as video surveillance. Moreover, we found that the PCT in the RLAB space produces the best natural color transfer and, at the same time, reduces the presence of noise. In future, this alternative approach to traditional night-vision methods could also be implemented in mobile applications.

APPENDIX

Equation sets for transforming coordinates from RGB to perceptual color spaces and backward.

A. $l\alpha\beta$ COLOR SPACE

Firstly, the data is transformed to an intermediate color space, the LMS.

$$\begin{bmatrix} L \\ M \\ S \end{bmatrix} = \begin{bmatrix} 0.3811 & 0.5783 & 0.0402 \\ 0.1967 & 0.7244 & 0.0782 \\ 0.0241 & 0.1288 & 0.8444 \end{bmatrix} \begin{bmatrix} R \\ G \\ B \end{bmatrix} \quad (21)$$

The data in the LMS color space show a large amount of skewness, which we can largely eliminate by converting data to a logarithmic space $\mathbf{L} = \log L$, $\mathbf{M} = \log M$ and $\mathbf{S} = \log S$ [56]. The equation used for the transformation of the LMS to the $l\alpha\beta$ space is

$$\begin{bmatrix} l \\ \alpha \\ \beta \end{bmatrix} = \begin{bmatrix} \frac{1}{\sqrt{3}} & 0 & 0 \\ 0 & \frac{1}{\sqrt{6}} & 0 \\ 0 & 0 & \frac{1}{\sqrt{2}} \end{bmatrix} \begin{bmatrix} 1 & 1 & 1 \\ 1 & 1 & -2 \\ 1 & -1 & 0 \end{bmatrix} \begin{bmatrix} \mathbf{L} \\ \mathbf{M} \\ \mathbf{S} \end{bmatrix}, \quad (22)$$

where the l axis corresponds to the luminance channel, and the α and β channels are chromatic yellow-blue and red-green opponent channels, respectively.

The corresponding inverse transformations are given next.

$$\begin{bmatrix} \mathbf{L} \\ \mathbf{M} \\ \mathbf{S} \end{bmatrix} = \begin{bmatrix} 1 & 1 & 1 \\ 1 & 1 & -1 \\ 1 & -2 & 0 \end{bmatrix} \begin{bmatrix} \frac{\sqrt{3}}{3} & 0 & 0 \\ 0 & \frac{\sqrt{6}}{6} & 0 \\ 0 & 0 & \frac{\sqrt{2}}{2} \end{bmatrix} \begin{bmatrix} l \\ \alpha \\ \beta \end{bmatrix}, \quad (23)$$

the pixel values are calculated as $L = \mathbf{L}^{10}$, $M = \mathbf{M}^{10}$ and $S = \mathbf{S}^{10}$. Finally, the conversion of data from LMS into RGB is given by the following equation

$$\begin{bmatrix} R \\ G \\ B \end{bmatrix} = \begin{bmatrix} 4.4679 & -3.5873 & 0.1193 \\ -1.2186 & 2.3809 & -0.1624 \\ 0.0497 & -0.2439 & 1.2045 \end{bmatrix} \begin{bmatrix} L \\ M \\ S \end{bmatrix}. \quad (24)$$

B. CIELUV AND CIELAB COLOR SPACES

The color space CIELUV is obtained from CIEXYZ using the following equations

$$u' = \frac{4X}{X + 15Y + 3Z}, \quad (25)$$

$$v' = \frac{9Y}{X + 15Y + 3Z}. \quad (26)$$

It is necessary to calculate the values u'_n and v'_n , which are the chromatic components of the reference white. In this

study, we use the illuminant E ($X_n = 1$, $Y_n = 1$ and $Z_n = 1$) as a reference white. Reinhard and Pouli [39] compared various reference whites and concluded that, the illuminant E is the best-suited for color transfer using perceptual spaces. The L^* , u^* and v^* components are computed applying the following equations

$$L^* = \begin{cases} (2/\sigma)^3 Y/Y_n & \text{if } Y/Y_n \leq \sigma^3 \\ 116(Y/Y_n)^3 - 16 & \text{otherwise,} \end{cases} \quad (27)$$

$$u^* = 13L^*(u' - u'_n), \quad (28)$$

$$v^* = 13L^*(v' - v'_n), \quad (29)$$

where $\sigma = 6/29$. For the inverse transformation from CIELUV to the CIEXYZ, the following equations are used.

$$u' = \frac{u^*}{13L^*} + u'_n, \quad (30)$$

$$v' = \frac{v^*}{13L^*} + v'_n, \quad (31)$$

$$Y = \begin{cases} Y_n L^*(\sigma/2)^3 & \text{if } L^* \leq 8 \\ Y_n \left(\frac{L^* + 16}{116} \right)^3 & \text{otherwise,} \end{cases} \quad (32)$$

$$X = Y \left(\frac{9u'}{4v'} \right), \quad (33)$$

$$Z = Y \left(\frac{12 - 3u' - 20v'}{4v'} \right). \quad (34)$$

The CIELAB color space is computed from CIEXYZ using Eqs. (35)–(38).

$$L^* = 116f(Y/Y_n) - 16, \quad (35)$$

$$a^* = 500 [f'(X/X_n) - f(Y/Y_n)], \quad (36)$$

$$b^* = 200 [f(Y/Y_n) - f(Z/Z_n)], \quad (37)$$

$$f(t) = \begin{cases} t^{1/3} & \text{if } t > \sigma^3 \\ t/(3\sigma^2) + 16/116 & \text{otherwise,} \end{cases} \quad (38)$$

where t can be X/X_n , Y/Y_n or Z/Z_n , and $\sigma = 6/29$.

For the inverse transformation, three intermediate variables are required, f_Y , f_X and f_Z , as shown in Eqs. (39)–(41),

$$f_Y = (L^* + 16)/166, \quad (39)$$

$$f_X = f_Y + (a^*/500), \quad (40)$$

$$f_Z = f_Y - (b^*/200). \quad (41)$$

Finally, Eqs. (42)–(44) are used to obtain the inverse transformation,

$$X = \begin{cases} X_n f_X^3 & \text{if } f_X > \sigma \\ f_X - 16/116 & \text{otherwise,} \end{cases} \quad (42)$$

$$Y = \begin{cases} Y_n f_Y^3 & \text{if } f_Y > \sigma \\ f_Y - 16/116 & \text{otherwise,} \end{cases} \quad (43)$$

$$Z = \begin{cases} Z_n f_Z^3 & \text{if } f_Z > \sigma \\ f_Z - 16/116 & \text{otherwise.} \end{cases} \quad (44)$$

REFERENCES

- [1] D.-H. Kim and E.-Y. Cha, "Intensity surface stretching technique for contrast enhancement of digital photography," *Multidimensional Syst. Signal Process.*, vol. 20, no. 1, pp. 81–95, 2009.
- [2] R. Firoz, M. S. Ali, M. N. U. Khan, M. K. Hossain, M. K. Islam, and M. Shahinuzzaman, "Medical image enhancement using morphological transformation," *J. Data Anal. Inf. Process.*, vol. 4, no. 1, p. 1, 2016.
- [3] G. Ginesu, D. D. Giusto, V. Margner, and P. Meinschmidt, "Detection of foreign bodies in food by thermal image processing," *IEEE Trans. Ind. Electron.*, vol. 51, no. 2, pp. 480–490, Apr. 2004.
- [4] X. Xie and K.-M. Lam, "Face recognition under varying illumination based on a 2D face shape model," *Pattern Recognit.*, vol. 38, no. 2, pp. 221–230, 2005.
- [5] L. Havasi, Z. Szlavik, and T. Sziranyi, "Detection of gait characteristics for scene registration in video surveillance system," *IEEE Trans. Image Process.*, vol. 16, no. 2, pp. 503–510, Feb. 2007.
- [6] A. R. Rivera, B. Ryu, and O. Chae, "Content-aware dark image enhancement through channel division," *IEEE Trans. Image Process.*, vol. 21, no. 9, pp. 3967–3980, Sep. 2012.
- [7] M. T. Sampson, "An assessment of the impact of fused monochrome and fused color night vision displays on reaction time and accuracy in target detection," Naval Postgraduate School, Monterey, CA, USA, Tech. Rep. AD-A321226, 1996.
- [8] M. A. Hogervorst and A. Toet, "Fast natural color mapping for night-time imagery," *Inf. Fusion*, vol. 11, no. 2, pp. 69–77, 2010.
- [9] Y. Rao, W. Lin, and L. Chen, "Image-based fusion for video enhancement of night-time surveillance," *Opt. Eng.*, vol. 49, no. 12, p. 120501-1–120501-3, 2010.
- [10] Y. Rao, W. Lin, and L. Chen, "Global motion estimation-based method for nighttime video enhancement," *Opt. Eng.*, vol. 50, no. 5, p. 057203-1–057203-6, 2011.
- [11] Y.-T. Kim, "Contrast enhancement using brightness preserving bi-histogram equalization," *IEEE Trans. Consum. Electron.*, vol. 43, no. 1, pp. 1–8, Feb. 1997.
- [12] E. D. Pisano et al., "Contrast limited adaptive histogram equalization image processing to improve the detection of simulated spiculations in dense mammograms," *J. Digit. Imag.*, vol. 11, no. 4, pp. 193–200, 1998.
- [13] E. F. Arriaga-Garcia, R. E. Sanchez-Yanez, J. Ruiz-Pinales, and M. de Guadalupe Garcia-Hernandez, "Adaptive sigmoid function bi-histogram equalization for image contrast enhancement," *J. Electron. Imag.*, vol. 24, no. 5, p. 053009, 2015.
- [14] T. Arici, S. Dikbas, and Y. Altunbasak, "A histogram modification framework and its application for image contrast enhancement," *IEEE Trans. Image Process.*, vol. 18, no. 9, pp. 1921–1935, Sep. 2009.
- [15] N. Xu, W. Lin, Y. Zhou, Y. Chen, Z. Chen, and H. Li, "A new global-based video enhancement algorithm by fusing features of multiple region-of-interests," in *Proc. IEEE Vis. Commun. Image Process. (VCIP)*, Nov. 2011, pp. 1–4.
- [16] Y. Chen, W. Lin, C. Zhang, Z. Chen, N. Xu, and J. Xie, "Intra-and-inter-constraint-based video enhancement based on piecewise tone mapping," *IEEE Trans. Circuits Syst. Video Technol.*, vol. 23, no. 1, pp. 74–82, Jan. 2013.
- [17] A. Gijssenij and T. Gevers, "Color constancy using natural image statistics and scene semantics," *IEEE Trans. Pattern Anal. Mach. Intell.*, vol. 33, no. 4, pp. 687–698, Apr. 2011.
- [18] E. Provenzi, C. Gatta, M. Fierro, and A. Rizzi, "A spatially variant white-patch and gray-world method for color image enhancement driven by local contrast," *IEEE Trans. Pattern Anal. Mach. Intell.*, vol. 30, no. 10, pp. 1757–1770, Oct. 2008.
- [19] J. Cepeda-Negrete and R. E. Sanchez-Yanez, "Automatic selection of color constancy algorithms for dark image enhancement by fuzzy rule-based reasoning," *Appl. Soft Comput.*, vol. 28, pp. 1–10, Mar. 2015.
- [20] V. Goffaux, C. Jacques, A. Mouraux, A. Oliva, P. Schyns, and B. Rossion, "Diagnostic colours contribute to the early stages of scene categorization: Behavioural and neurophysiological evidence," *Vis. Cognit.*, vol. 12, no. 6, pp. 878–892, 2005.
- [21] A. Toet and J. Walraven, "New false color mapping for image fusion," *Opt. Eng.*, vol. 35, no. 3, pp. 650–659, 1996.
- [22] A. Toet, "Natural colour mapping for multiband nightvision imagery," *Inf. Fusion*, vol. 4, no. 3, pp. 155–166, 2003.
- [23] A. Toet and E. M. Franken, "Perceptual evaluation of different image fusion schemes," *Displays*, vol. 24, no. 1, pp. 25–37, 2003.
- [24] Y. HaCohen, E. Shechtman, D. B. Goldman, and D. Lischinski, "Non-rigid dense correspondence with applications for image enhancement," *ACM Trans. Graph.*, vol. 30, no. 4, pp. 70:1–70:10, 2011.
- [25] A. Levin, D. Lischinski, and Y. Weiss, "Colorization using optimization," *ACM Trans. Graph.*, vol. 23, no. 3, pp. 689–694, 2004.
- [26] D. Cohen-Or, O. Sorkine, R. Gal, T. Leyvand, and Y.-Q. Xu, "Color harmonization," *ACM Trans. Graph.*, vol. 25, no. 3, pp. 624–630, 2006.
- [27] C. Sauvaget, J.-N. Vittaut, J. Suarez, V. Boyer, and S. Manuel, "Automated colorization of segmented images based on color harmony," *J. Multimedia Process. Technol.*, vol. 1, no. 4, pp. 228–244, 2010.
- [28] E. Reinhard, M. Adhikhmin, B. Gooch, and P. Shirley, "Color transfer between images," *IEEE Comput. Graph. Appl.*, vol. 21, no. 5, pp. 34–41, Sep./Oct. 2001.
- [29] X. Xiao and L. Ma, "Color transfer in correlated color space," in *Proc. ACM Int. Conf. Virtual Reality Continuum Appl.*, 2006, pp. 305–309.
- [30] A. Abadpour and S. Kasaei, "An efficient pca-based color transfer method," *J. Vis. Commun. Image Represent.*, vol. 18, no. 1, pp. 15–34, 2007.
- [31] C. R. Senanayake and D. C. Alexander, "Colour transfer by feature based histogram registration," in *Proc. Brit. Mach. Vis. Conf.*, 2007, pp. 1–10.
- [32] T. Pouli and E. Reinhard, "Progressive color transfer for images of arbitrary dynamic range," *Comput. Graph.*, vol. 35, no. 1, pp. 67–80, 2011.
- [33] N. Papadakis, E. Provenzi, and V. Caselles, "A variational model for histogram transfer of color images," *IEEE Trans. Image Process.*, vol. 20, no. 6, pp. 1682–1695, Jun. 2011.
- [34] S. Liu, H. Sun, and X. Zhang, "Selective color transferring via ellipsoid color mixture map," *J. Vis. Commun. Image Represent.*, vol. 23, no. 1, pp. 173–181, 2012.
- [35] X. Qian, Y. Wang, and B. Wang, "Effective contrast enhancement method for color night vision," *Infr. Phys. Technol.*, vol. 55, no. 1, pp. 130–136, 2012.
- [36] X. Qian, L. Han, Y. Wang, and B. Wang, "Color contrast enhancement for color night vision based on color mapping," *Infr. Phys. Technol.*, vol. 57, pp. 36–41, Mar. 2013.
- [37] A. Toet and M. A. Hogervorst, "Progress in color night vision," *Opt. Eng.*, vol. 51, no. 1, p. 010901, 2012.
- [38] E. A. Essock, M. J. Sinai, J. S. McCarley, W. K. Krebs, and J. K. DeFord, "Perceptual ability with real-world nighttime scenes: Image-intensified, infrared, and fused-color imagery," *Hum. Factors*, vol. 41, no. 3, pp. 438–452, 1999.
- [39] E. Reinhard and T. Pouli, "Colour spaces for colour transfer," in *Proc. Int. Workshop Comput. Color Imag.*, 2011, pp. 1–15.
- [40] B. Jiang et al., "Nighttime image dehazing with modified models of color transfer and guided image filter," in *Multimedia Tools and Applications*. New York, NY, USA: Springer, 2017, pp. 1–17, doi: 10.1007/s11042-017-4954-9.
- [41] Y. Zheng and E. A. Essock, "A local-coloring method for night-vision colorization utilizing image analysis and fusion," *Inf. Fusion*, vol. 9, no. 2, pp. 186–199, 2008.
- [42] S. Yin, L. Cao, Y. Ling, and G. Jin, "One color contrast enhanced infrared and visible image fusion method," *Infr. Phys. Technol.*, vol. 53, no. 2, pp. 146–150, 2010.
- [43] Y.-J. Wang, H.-K. Qiu, L.-L. Wang, and X.-B. Shi, "Research on algorithm of night vision image fusion and colorization," *J. China Univ. Posts Telecommun.*, vol. 20, pp. 20–24, Aug. 2013.
- [44] M. Fairchild, "Refinement of the LAB color space," *Color Res. Appl.*, vol. 21, pp. 338–346, Jun. 1996.
- [45] J. Yin and J. R. Cooperstock, "Color correction methods with applications to digital projection environments," *J. WSCG*, vol. 12, nos. 1–3, pp. 499–506, 2004.
- [46] Y. Xiang, B. Zou, and H. Li, "Selective color transfer with multi-source images," *Pattern Recognit. Lett.*, vol. 30, no. 7, pp. 682–689, 2009.
- [47] J. Schanda, Ed., *Colorimetry: Understanding the CIE System*. Hoboken, NJ, USA: Wiley, 2007.

[48] M. Stokes, M. Anderson, S. Chandrasekar, and R. Motta, "A standard default color space for the Internet-sRGB," Hewlett-Packard, Microsoft, Palo Alto, CA, USA, Tech. Rep. IEC 61966-2-1, 1996.

[49] Y. Rubner, C. Tomasi, and L. J. Guibas, "The earth mover's distance as a metric for image retrieval," *Int. J. Comput. Vis.*, vol. 40, no. 2, pp. 99–121, Nov. 2000.

[50] A. Bhattachayya, "On a measure of divergence between two statistical populations defined by their probability distribution," *Bull. Calcutta Math. Soc.*, vol. 35, no. 1, pp. 99–109, 1943.

[51] D. Martin, C. Fowlkes, D. Tal, and J. Malik, "A database of human segmented natural images and its application to evaluating segmentation algorithms and measuring ecological statistics," in *Proc. 8th IEEE Int. Conf. Comput. Vis. (ICCV)*, vol. 2, Jul. 2001, pp. 416–423.

[52] W. B. Thompson, P. Shirley, and J. A. Ferwerda, "A spatial post-processing algorithm for images of night scenes," *J. Graph. Tools*, vol. 7, no. 1, pp. 1–12, 2002.

[53] J. Cepeda-Negrete. *Personal Website*. Accessed: Sep. 21, 2017. [Online]. Available: <https://jonathancn16.wixsite.com/profile>

[54] J. Cepeda-Negrete. *Academic Website*. Accessed: Sep. 21, 2017. [Online]. Available: <https://www.diciva.ugto.mx/profesores/jonathancepeda.html>

[55] K. Tsirikolias, "Low level image processing and analysis using radius filters," *Digit. Signal Process.*, vol. 50, pp. 72–83, Mar. 2016.

[56] D. L. Ruderman, T. W. Cronin, and C.-C. Chiao, "Statistics of cone responses to natural images: Implications for visual coding," *J. Opt. Soc. Amer. A, Opt. Image Sci.*, vol. 15, no. 8, pp. 2036–2045, 1998.



JONATHAN CEPEDA-NEGRETE received the bachelor's degree in engineering of communications and electronics and the master's and Ph.D. degrees in electrical engineering from the University of Guanajuato, Mexico, in 2011, 2012, and 2016, respectively. He is a full-time Professor with the Department of Agricultural Engineering, Life Sciences Division, University of Guanajuato, Irapuato, Gto. His current research interests include computer vision applications, mainly color image processing, pattern recognition, and computer graphics.



computational intelligence applications in feature extraction and decision making.

RAUL E. SANCHEZ-YANEZ (M'91) received the B.E. degree in electronics and the master's degree in electrical engineering from the Universidad de Guanajuato and the D.Sc. degree in optics from the Centro de Investigaciones en Óptica, Leon, Mexico, in 2002. He has been a full-time Professor with the the Engineering Division of the Irapuato-Salamanca Campus, Universidad de Guanajuato, since 2003. His research interests include color and texture analysis for computer vision and



FERNANDO E. CORREA-TOME received the B.E. degree in communications and electronics and the M.E. and D.E. degrees in electrical engineering from the Universidad de Guanajuato, Mexico, in 2009, 2011, and 2015, respectively. His current research interests include image and signal processing, pattern recognition, computer vision, and machine learning.



extraction and decision making.

ROCIO A. LIZARRAGA-MORALES (M'09) received the B.Eng. degree in electronics from the Instituto Tecnológico de Mazatlan in 2005 and the M.Eng. and D.Eng. degrees in electrical engineering from the Universidad de Guanajuato, Mexico, in 2009 and 2014, respectively. She is currently an Associate Professor with the Universidad de Guanajuato. Her main research interests include color and texture analysis for computer vision tasks, and computational intelligence applications in feature

...